Influence of alpha- and gamma- cyclodextrin lipophilic derivativeson curcumin-loaded SLN

Influence of α- and γ- cyclodextrin lipophilic derivatives on curcumin-loaded SLN

Daniela Chirio, Marina Gallarate*, M. Trotta, M.E. Carlotti
Emanuela Calcio Gaudino, Giancarlo Cravotto

Dipartimento di Scienza e Tecnologia del Farmaco, Università di Torino, via P. Giuria 9, 10125 Torino.

**Author for correspondence: E-mail: marina.gallarate@unito.it; FAX +39.011.6707687*

Key words: alkylated cyclodextrins, solid lipid nanoparticles, curcumin, synthesis.

ABSTRACT

Solid lipid nanoparticles (SLN) made of different triglycerides (TG) in the presence and in the absence of various modified α- and γ-cyclodextrins (CD) were prepared by the solvent injection technique. A new synthesis of lipophilic derivatives of γ- CD was developed in this work.
Curcumin (CU), a natural polyphenol with antitumor, antioxidant and anti-inflammatory properties, was used as model drug. SLNs mean sizes were in the 250-800 nm range and afforded CU entrapment efficiency in the 12-85% range. The presence of CD derivatives with almost the same chain length of TG induced an improvement of nanoparticle characteristics decreasing mean size values and increasing CU entrapment efficiency.
A significant reduction in CU photodegradation was noted only when the drug was vehicled in tristearin-SLN, which became less pronounced in the presence of CD-derivatives, determining a loss in photoprotection.
The hydrolytic stability of curcumin was highly improved by drug loading in tristearin-SLN, and only slightly by loading it in tricaprin-SLN, and this seemed not to be influenced by the presence of CD derivatives.
Skin uptake studies revealed an increase in CU skin accumulation when CU was loaded in SLN obtained with all CD derivatives, particularly with most lipophilic one.

INTRODUCTION

Curcumin (CU), a hydrophobic natural polyphenol isolated from *Curcuma longa*, has been used for centuries in indigenous medicine for the treatment of a variety of inflammatory conditions [1]. It exhibits a wide range of pharmacological capacities, including antitumor, antioxidant, anti-inflammatory, antimicrobial activities [2]. Its most interesting potential use is probably against cancer: pre-clinical studies have shown that it can inhibit cancerogenesis in a variety of cell lines, including breast, cervical, colon, gastric, hepatic, oral epithelial, ovarian, pancreatic, prostate cancer and leukaemia [3]. In addition, it was reported that CU caused cell death in eight melanoma cell lines, also in those carrying mutant p53, that are very resistant to conventional chemotherapy [4]. The main drawbacks for clinical applications of CU are its low water solubility at acidic and physiological pH and its rapid hydrolysis under alkaline conditions to yield ferulic acid, its methyl ester and vanillin [5]. It is also very susceptible to photochemical degradation [6]. Moreover, studies on its absorption, distribution, metabolism and excretion have revealed that its poor absorption and rapid metabolism severely curtail its bioavailability [7]. These hurdles can be met by incorporating CU into nanoparticles, liposomes, micelles or complexing it with cyclodextrins (CD) in aqueous solutions. Solid lipid nanoparticles (SLN) loaded with curcuminoids for topical administration were developed and characterised by Tiyaboonchai et al [8]. SLN with a mean size of 450 nm were found to be stable for 6 months and incorporation into SLN strongly reduced the light and oxygen sensitivity of curcuminoids.

Li et al [9] investigated the antitumor activity of liposome-carried CU against human pancreatic carcinoma cell. They found that liposomal CU inhibited pancreatic carcinoma growth and exhibited antiangiogenic effects; however, a proper comparison of the effect of liposomal CU with that of free CU and of the respective biodistribution profiles has yet to be carried out to confirm the enhancement of CU bioavailability by liposomal CU.

Some Authors [10] compared the intestinal absorption of plain CU and of a micellar CU formulation with phospholipids and bile salt using an *in vitro* model; respective absorption rates were 47% and 56%. Polymeric micelles studied in rats by Ma et al [11] afforded a 60-fold increase of CU half-life compared to that of plain CU. These results suggested that micelles can improve the gastrointestinal absorption of drugs resulting in higher plasma levels and slow down drug elimination with a net improvement in bioavailability.

Recently, the Tønnesen group [12] complexed CU with CD to improve its water solubility and its stability to hydrolysis and photochemical attack. Complex formation increased water solubility at

pH 5 by a factor of at least 10^4. The stability of CU to hydrolysis under alkaline conditions was likewise strongly improved, while the photodecomposition rate was increased compared to that of CU when dissolved in organic solvents. The cavity size of the CD, also the charge and bulkiness of its side-chains influenced stability constant for complexation and the degradation rate of CU.

Several authors described the aggregation properties of CDs bearing hydrophobic substituents in aqueous media [13], showing that they can form a variety of self-organized structures, such as micelles, vesicles, and mono- or multilayers [14].

The aim of the present work was to produce triglyceride-based, CU-loaded SLN by the solvent injection method, a simple, quite inexpensive technique originally developed with liposomes. Several hydrophobic derivatives of α- and γ-CD were synthesised and mixed with tryglycerides (TG) to ascertain how the presence of CDs may affect the physico-chemical properties of SLNs and their drug-entrapment efficiency, as well as their stability over time. Moreover, in view of the well-known antioxidant and anti-free-radical activity of CU, a possible cutaneous use of CU-loaded SLN was hypothesised and preliminary *in vitro* permeation studies through ear-pig skin were carried out.

EXPERIMENTAL

Materials

CU was supplied by Sigma (St. Louis, USA), α- and γ-cyclodextrin, hexanol, octanol, decanol, dodecanol, tetradecanol, hexadecanol, carbonyldiimidazole, tricaprin (TC), trilaurin (TL), trimyristin (TM), tripalmitin (TP) and tristearin (TS) were purchased from Fluka (Buchs, Switzerland), Myritol®318 (caprylic-capric triglyceride) was provided by Merck (Whitehouse Station, USA), 98% hydrolysed PVA 14000-21000 MW (PVA 14000) was from BDH Chemicals (Poole, England). Deionised water was obtained by a MilliQ® system (Millipore, Bedford, MO, USA). All other reagents were of analytical grade and obtained from Carlo Erba (Milan, Italy).

Instruments

NMR spectra were recorded on a Bruker Avance 300 using as internal reference the deuterated solvent. The IR spectra were recorded on a Shimadzu FT-IR 8001 spectrophotometer; ESI mass spectra were recorded on a Waters Micromass ZQ with ESI sources. Analytical TLC (Thin Layer Chromatography) was carried out using plates from Merck (Alufolien, F_{254}, 0.25 mm); spots were visualised by heating after the plates had been sprayed with 5% sulphuric acid in ethanol; microscopic observations were performed using a DM 2500 optical microscope equipped with a fluorescent lamp (Leica); Laser Light Scattering measurements were done by 90 Plus Particle Size

Analyzer (Brookhaven); HPLC analysis was performed using a Shimadzu (Kyoto, Japan) chromatograph equipped with a LC-10AD pump unit and with an SPD-2A ultraviolet detector; centrifugations were obtained by Allegra 64R Centrifuge (Beckman Coulter); DSC was performed with a DSC7 differential scanning calorimeter (Perkin Elmer); photodegradation studies were performed using a TL 40/12 RST40T12 (Philips) UVA lamp.

Synthesis of alkylcarbonate-γ-CD derivatives

We synthesised alkylcarbonates γ-CD derivatives with chain lengths of 6 to 16 carbon atoms (C6γ-CD - C16γ-CD) according to a procedure reported in the literature [15]. Briefly, the alkyl alcohol was activated by reaction with an excess of carbonyldiimidazole in alcohol-free chloroform. Successively the imidazoyl derivative was allowed to react with anhydrous γ-CD in anhydrous pyridine at 80°C for 4 hours. Once the reaction was over, distilled water was added and the precipitate was recovered by filtration, washed many times with water and lyophilised.

General procedure for the synthesis of monoacyl-α-CD derivatives.

In a 50 ml three-necked round-bottomed flask equipped with a magnetic stirrer and addition funnel, α-CD (1 g, 1.028 mmol), 4-dimethylaminopyridine (6.2 mg, 0.051 mmol) and triethylamine (0.42 g, 4.14 mmol) were dissolved in dry DMF (5 ml). The solution was cooled down to -15°C and the acyl chloride (1.5 eq), previously diluted with DMF (2 ml) was added dropwise under stirring over a period of 5 min. The reaction mixture was stirred for 2 h at 0°C, then another 8 h at room temperature, and finally filtered on a sintered glass funnel to remove triethylammonium chloride.

Work-up for monoisostearoyl-α-CD (C18α-CD)

The resulting solution was diluted with EtOAc and washed three times with 0.5% HCl, then with a saturated solution of K_2CO_3, and finally dried over sodium sulphate. After solvents were removed under vacuum in kugelrohr, 0.458 g of **1** were obtained (yield 36%).

FTIR (KBr): 2926, 2856, 1736, 1659, 1153, 1080, 949, 704 cm^{-1}.

^{1}H-NMR (DMSO-d_6, 300 MHz,) δ 5.57 (m, 12 H, 2,3-O*H*), 4.85 (m, 6H, 1-H), 4.53 (m, 5H, 6-O*H*), 3.84-3.62 (os, 36H, 2,3,4,5,6$_a$,6$_b$-H), 2.36 (m, 2H, 2-H $_{isost}$), 1.29 (m, -C*H*,-C*H*$_{2\ isost}$), 0.88 (t, J=7.2, 6H, -C*H*$_{3\ isost}$). ESI-MS (m/z): 1240 [M^++H].

Work-up for monoundecenoyl-α-CD (C11 α-CD)

The solution was diluted with acetone and kept under magnetic stirring at 4°C overnight. The resulting suspension was centrifuged (2,500 rpm), the sediment washed with EtOH (20 ml x 3) and dried under vacuum. 0.288 g of **2** were obtained (24.7%).

FTIR (KBr): 2928, 2856, 1641, 1458, 1365, 1289, 1153, 1078, 949, 862, 704 cm^{-1}.

^{1}H-NMR (DMSO-d_6, 300 MHz) δ 5.83-5.72 (m, 1H, 10'-H), 4.95 (dd, J=1.5, 2H, 11'-H), 4.79 (d, J=2.7, 6H,1-H), 4.35 (dd, J=3.3, 1H, 6*a*-H est), 3.79-3.59 (os, 24H, 3,4,5,6*b*-H), 3.28 (m, 6H, 2-H), 2.16 (t, J=7.2, 2H, 2'-H), 2.0 (q, J=6.6, 2H, 9'-H), 1.47 (m, 2H, 3'-H), 1.23 (m, 10H, 4',5',6',7',8'-H).

ESI-MS (m/z): 1177 [M^++K].

Preparation of TG-SLNs and TG/CD derivatives-SLNs

CU-loaded SLNs were prepared by the solvent injection technique [16]. Different TG –TC, TL, TM, TP and TS– (100 mg/ml) and CU (5 mg/ml) were dissolved by heat (from 32 to 55°C depending on the TG) in 0.2 ml DMSO. Each solution was added dropwise to 4ml 1% w/V PVA 14000 aqueous solution being irradiated in a ultrasound bath at 25 ± 1°C. By the same technique the following SLNs were also prepared:

- TL-SLN using 3:1 (w:w) TL/C6-C8-C10-C12-C14-C16γ-CD mixtures
- different TG-SLN using 3:1 (w:w) TG/C11-C18 α-CD mixtures
- different TG-SLN using 3:1 (w:w) TG/CD derivatives with the same chain lengths

Physico-chemical characterisation of CU-loaded SLN

The morphology of SLN dispersions and the localisation of CU in them was determined using the optical microscope equipped with a fluorescent lamp. A drop of SLN dispersion was directly observed under fluorescent light and analysed by an image analysis program (Motic Inc., Hong Kong).

SLN sizes and polydispersity indexes were determined by laser-light scattering. Measurements were obtained at an angle of 90° and at 25 ± 1°C. Scattering intensity data were analysed by a digital correlator and fitted by the method of inverse Laplace transformation. Dispersions were diluted 1:100 with water immediately before LLS analysis and all measurements were made in triplicate.

Determination of CU entrapment efficiency (EE)

1 ml of the SLN suspension was centrifuged for 30 min at 24000 rpm. The sediment was washed twice with 1 ml ethanol/water 30/70 (V:V) to eliminate adsorbed CU; the solid residue was dissolved in 1 ml ethanol and opportunely diluted and analysed by HPLC.

HPLC analytical conditions were: column: Allsphere ODS-2 (150 × 4.6 mm); mobile phase: methanol:water:acetic acid 70:30:1; flow rate: 1 ml min^{-1}; retention time: 5.5 min; λ: 450 nm.

EE was expressed as CU amount in washed SLN vs total CU amount in 1ml SLN suspension × 100.

DSC analysis

Experimental conditions.

Samples were placed in conventional aluminium pans and a scan speed of 2°C min^{-1} was used operating in the appropriate temperature range.

Systems under study

TL transition peak: TL, TL-C6γ-CD, TL-C10γ-CD, TL-C12γ-CD, TL-C16γ-CD, TL-C11α-CD SLN were analysed: 13 μl SLN samples were used.

CU transition peak: CU, CU:C11α-CD complexes at 1:2 and 1:4 molar ratio, CU:C11α-CD physical mixture at 1:2 molar ratio, ratio, CU:C18α-CD complexes at 1:2 and 1:4 molar ratio, CU:C18α-CD physical mixture at 1:2 molar ratio, CU:C12γ-CD complexes at 1:2 and 1:4 molar ratio, CU:C11α-CD physical mixture at 1:2 molar ratio were analysed.

Complexes were prepared as follows: appropriate amounts of CD derivatives and CU were dispersed/solubilised in ethanol. The organic solvent was then removed by keeping the suspension under a nitrogen stream for 30 min.

NMR analysis

^{1}H-NMR spectra of both CU and its complexes with C_{11}α-CD and C_{18}α-CD (1:2 and 1:4 molar ratio) were performed in DMSO-d6 (300 MHz). Table 1 shows chemical shifts of CU and that of the complexes as well as the relative shifts due to the interaction with the CDs.

	CU δ (ppm)	**αCD-C_{11}/CU (2:1)**		**αCD-C_{11}/CU (4:1)**		**αCD-C_{18}/CU (2:1)**		**αCD-C_{18}/CU (4:1)**	
		Δ (ppm)	δ (ppm)	**Δ** (ppm)	δ (ppm)	**Δ** (ppm)	δ (ppm)	**Δ** (ppm)	δ (ppm)
s, 2H, 8-OH	9.65	-	-	-	-	-	-	-	-
d, J=15.9, 2H, 4-H	7.55	-0.013	7.54	-0.027	7.52	-0.005	7.55	+0.015	7.57
d, J=1.5, 2H, 6-H	7.32	-0.015	7.31	-0.022	7.30	-0.005	7.32	+0.022	7.34
dd, J_3=8.1-J_4=1.5, 2H, 10-H	7.15	-0.016	7.14	-0.025	7.13	-0.005	7.15	+0.021	7.17
d, J_3=8.1, 2H, 9-H	6.82	+0.020	6.84	+0.011	6.83	-0.005	6.82	+0.026	6.85
d, J=15.9, 2H, 3-H	6.75	-0.008	6.74	-0.021	6.73	-0.005	6.75	+0.025	6.77
s, 1H, 1-H	6.06	-0.004	6.05	-0.017	6.04	-0.005	6.06	+0.022	6.08
s, 6H, 7-OCH_3	3.84	-0.008	3.83	-0.015	3.83	-0.005	3.83	+0.019	3.86

Curcumin photostability

Experimental conditions.

Photodegradation of CU was studied by UVA in the 320-400 nm range. Samples (2 ml each) were introduced in hermetically screwed Pyrex glass cells placed at 10 cm from the light source and maintained under continuous stirring . In such conditions the radiation power per surface unit was $8.9 \cdot 10^{-4}$ W cm^{-2}. Every 30 min for a total 3 hour irradiation, 100 µl of each sample was dissolved by 400 µl DMSO and analysed by HPLC. During a 3-hour irradiation run, the total dose of UV was 9.61 J cm^{-2}. All experiments were carried out in triplicate.

Systems under study.

Free CU: CU suspension in 0.1 M PBS pH 6.0

CU - loaded SLN: TC, TC–C10γ-CD, TC–C11α-CD, TS, TS–C18α-CD SLNs dispersed in 0.1 M PBS pH 6.0

In all systems CU concentration was $5.0 \cdot 10^{-5}$ M.

Curcumin hydrolytic stability

Experimental conditions.

Stability of CU to hydrolysis was investigated in 0.1 M phosphate buffer (pH 7.4). Samples (2 ml each) were kept under magnetic stirring at 37 ± 1°C. At 30 min intervals for a total of 3 hours, 100 µl of each sample were dissolved by 400 µl DMSO and analysed by HPLC. All studies experiments were carried out in triplicate.

Samples under study.

Free CU: CU suspension in 0.1 M PBS pH 7.4

SLN-loaded CU: TC, TC–C10γ-CD, TC–C11α-CD, TS, TS–C18α-CD SLNs dispersed in 0.1 M PBS pH 7.4

In all systems CU concentration was $5.0 \cdot 10^{-5}$ M.

In vitro transepidermal permeation and skin uptake experiments

Experimental conditions.

CU transepidermal permeation and skin uptake were determined using a vertical Franz cell [16] and 1.2 mm-thick pig ear skin. The skin was rinsed with normal saline to maintain an *in vivo* transepidermal hydration gradient [17] and was pre-hydrated by floating, stratum corneum upward, on 0.002% w/v aqueous sodium azide. The receptor chamber of the cell was filled with 6 ml 1% w/V PVA 14000 aqueous solution. The samples to be tested were applied to the skin surface, which had an available diffusion area of 2.05 cm^2, and left to dry out. The content of the receptor chamber, being continuously stirred at 37 ± 1°C, was removed at appropriate intervals for CU determination

while the cell was immediately refilled with fresh receptor solution. At the end of the permeation experiments (24 h) the skin surface was washed five times with 1% w/V PVA 14000 to remove excess drug. The skin was then cut into small pieces, added of 3 ml ethanol and left under continuous stirring for 3 hours at room temperature. After 5 min centrifugation at 5000 rpm, CU content in the upper phase was determined by HPLC. All experiments were carried out in triplicate.

Systems under study.

Free CU: CU solution in Myritol®318

SLN-loaded CU suspension: TC, TC–C10γ-CD, TC–C11α-CD, TS, TS–C18α-CD SLNs dispersed in 1% w/V PVA 14000

Solid SLN-loaded CU: TC, TC–C10γ-CD, TC–C11α-CD, TS, TS–C18α-CD SLNs.

In all systems CU concentration was $5.0 \cdot 10^{-5}$ M.

RESULTS AND DISCUSSION

Synthesis of monoacyl-α-CD derivatives

Because of the similar reactivity of the hydroxyl groups, it is difficult to effect selective monosubstitution of CDs, and multistep group transfer strategy based on protection/deprotection is required. Tong et al. [18] and Rao et al. [19] utilised basic catalysis to prepare monosubstituted β-CD derivatives directly, but the reaction conditions were complex and required precise pH control. As compared with conventional chemical catalysis, enzyme catalysis often allows higher selectivity under milder conditions [20]. In the case of α-CD we could achieve selective monoacylation with acyl chloride in DMF under a strict control of the temperature (from -15°C to 0°C, then r.t.). The different solubility in water between monoacyl-α-CD derivatives and native α-CD facilitates the work-up and the recovery of pure the products **1** and **2** in acceptable yields (Scheme 1). Bidimensional NMR-studies showed that the main product in both cases is the monoacyl derivative in position 6.

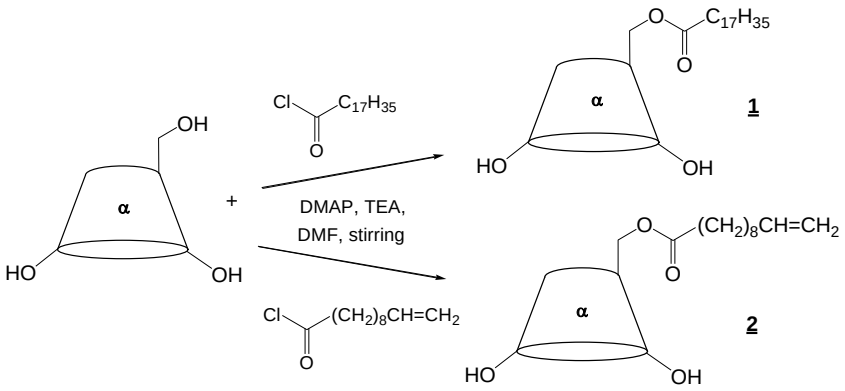

Scheme 1. General scheme of the synthetic procedure

CD derivatives and their 2:1 and 4:1-complexes with CU were fully characterized mainly by NMR that showed major interactions in 4:1- complexes as reported in the corresponding columns in Table 1 (Δ ppm).

Physicochemical characterisation of CU-loaded SLN

By the solvent-injection technique we could obtain CU-loaded SLN with all of the selected TGs, as well as in the presence of lipophilic derivatives of α- and γ-CD. Mean diameters of all SLNs were in the 250-800 nm range, as reported in Tables 1, 2 and 3.

Table 1 reports mean diameters and polydispersion indexes of TL-SLN prepared with and without different alkyl derivatives of γ-CD. As we see, derivatives of shorter chain length induced an increase of mean diameters while CD derivatives with almost the same chain length as TL (C10γ-CD and C12γ-CD) induced an evident decrease in SLN mean size values (up to 237 nm). This effect might be due to the surface activity of CD derivatives, becoming manifest for chain lengths of 10 up to 14 carbon atoms [21], but decreasing for longer chains (C16-C18) owing to their poor water solubility. Another possible explanation of SLN size decrease could be a greater affinity between the TL molecule and the CD derivative with the same chain length. To verify this hypothesis, SLNs of different TGs were prepared in the absence and in the presence of C12γ-CD and of CD derivatives having the same chain length as the corresponding TG. Results are reported in Table 2. As we see, a decrease in SLN mean size mainly occurred when the CD having the same chain length as the TG was present in SLNs. This effect was particularly evident in TC- and TM-SLN, while it was less pronounced in the case of TP, probably as a consequence of the poor water solubility of C16γ-CD.

SLN were also prepared in the presence of C11 and C18 mono-derivatives of α-CD. In Table 3 mean sizes and polydispersion indexes of these SLN are reported. Also the presence of α-CD derivatives in TG-SLN determined a decrease of nanoparticle size, confirming the role of TG-CD in influencing SLN dimensions. Compared to γ-CD derivatives, the influence of α-CD derivatives was not so marked, particularly in the case of C11α-CD, probably because the presence of a single alkyl chain reduces its interaction with the TG lipid matrix of SLN. The decrease in SLN mean sizes was particularly evident when C18α-CD was introduced in the TS-SLNs, indicating a stronger interaction between TG and CD derivatives with the same chain length.

Due to the low dimension of SLN prepared, the optical microscope analysis revealed the presence of dotted-like particles which confirmed the results obtained with LLS. Fig 1a and 1b show TL and TL-C12γ-CD SLN respectively as examples. The use of a fluorescent lamp made it easy to localize within the SLNs CU, a compound that is endowed with natural fluorescence. Figures 2a and 2b illustrates CU-charged TL and TL-C12γ-CD SLNs respectively, showing that CU was located in spherical particles, probably SLNs.

Determination of CU entrapment efficiency

SLNs were also characterised by the percent of encapsulated CU, i.e., the entrapment efficiency (EE). In Table 4 CU EE is reported for TL-SLNs with and without the addition of γ-CD derivatives having different chain lengths. CU EE in TL-SLNs exceeded 60%; the introduction of CD derivatives with shorter chain lengths caused an evident decrease in EE (up to 12% in the presence of C6γ-CD), while a marked increase of EE occurred when C12γ-CD was used. The stronger interaction occurring between TG and CD derivatives with the same chain length, that was hypothesised as a probable cause of SLN mean size decrease, might also determine a higher CU EE (up to 80%). The encapsulation of CU seems to be related to the interaction of CD with TG in SLN: probably, a tighter assembly of CD derivatives within the lipid matrix could cause both size reduction and CU entrapment increase. A similar behaviour was observed also with other TG-SLNs: in Table 5 CU EE is reported for SLNs of different TG either alone, or in the presence of C12γ-CD or of γ-CD matching each TG in chain length. The presence of the γ-CD derivatives always determined an increase in the percentage of CU entrapped, which was particularly marked (up to 30% or higher) when the CD had the same chain length as the TG. When C11α-CD and C18α-CD (Table 6) were used as components of TG-SLNs, two different pictures emerged. When the CD chain length was close to that of the TG present in SLN, a significant increase of CU EE (up to 25%) was seen. On the contrary, the presence of CD derivatives with chain lengths that were quite different from that of the TG caused a significant decrease of CU EE. This result is apparently in contrast with that obtained with derivatives of γ-CD (reported in Table 5): here the addition of C12γ-CD always determined an increase in CU entrapment, probably because, the lipophilicity of a trisubstituted CD being higher than that of a monosubstituted one, the former one had a more pronounced affinity for lipid aggregates.

DSC analysis

DSC analysis was used both to ascertain the formation of CU inclusion complexes and to evaluate the interaction between TG and CD derivatives.

Figure 3 shows thermograms evidencing complex formation. Complexes of CU and C11α-CD, C18α-CD and C12γ-CD were respectively studied. The transition peak of CU occurred at 44.4°C; when physical mixtures of CU and a CD were analyzed, a marked reduction in transition enthalpies was noted, even if a broader peak was still present. This indicates that a certain interaction occurred when the substances were mixed together in the solid state.

When CU:CD complexes, prepared as described in methods section, were analysed instead, different pictures were seen. In the case of C12γ-CD, the peak disappeared completely for a 2:1 CD:CU molar ratio, probably indicating a complete inclusion of the drug in the CD cavity. With C11α-CD and C18α-CD complexes, a higher CD:CU molar ratio (4:1) was required to cause the disappearance of the peak. From these results we can hypothesise that CU fits better the γ-CD cavity, which is larger than that of α-CD.

Taking into account these observations and re-considering CU entrapment efficiencies in TG-SLNs in the presence of C12γ-CD (Table 5) and C18α-CD (Table 6), we can partially explain the different trends noted. When a γ-CD derivative was introduced, usually, a certain increase in EE was found, independently of TG chain length even if the highest EE were noted when TG and CD derivatives had the same chain length; on the contrary, when C18α-CD was incorporated an enhancement in EE occurred only in the case of TS. The higher affinity of γ-CD derivatives for CU seems therefore also to hold in lipidic nanoparticulate systems.

DSC was also employed to investigate the solid state of nanoparticles and to explore interactions between lipid matrices and CD derivatives.

Thermograms of different TL-SLNs are reported in Fig. 4. TL-SLNs showed a sharp melting peak at 44.41°C, a temperature just below the melting point of plain TL which is 46.40°C: according to literature data [22] the lower melting point of colloidal systems can be due to the small dimensions of the particles, in particular to their large surface to volume ratio, as well as to the presence of impurities, surfactants and stabilizers. All TL-γ-CD and TL-C11α-CD SLNs have melting points that are lower than that of TL-SLN, indicating that interaction between CD-derivatives and TL occurred in SLNs. Even if it is difficult to quantify the strength of each interaction, it is noteworthy that the transition enthalpy of TL (66.01 J g^{-1}) was dramatically reduced in the presence of all CD derivatives (up to ten times for TL-C10γ-CD SLNs), excepting the case of C6-γ-CD, for which the decrease was only 20%. These results seem to further confirm the interactions occurring between TL and CD derivatives in SLN.

Curcumin photostability

Considering the well-known antioxidant and antiradical activity of CU [23-24], a possible dermatologic and cosmetic use of CU-loaded SLNs was envisaged.

Experiments were in order to evaluate the UV photodegradation that CU is liable to undergo in a topical formulation after application to the skin. In this study we examined SLNs prepared with TC and TS, triglycerides with the lowest and the highest melting point in the series under study (31-32°C and 72-75°C respectively); in particular, a TC-SLN could be considered as a lipid particle which can melt at the temperature of skin surface. This melting might determine a rather release of CU from the lipid matrix itself, probably determining a highly concentrated layer of drug on skin surface.

In Figure 5, UV degradation curves are reported for all the systems under study. When suspended in PBS pH 6, CU underwent a rapid degradation, as only 10% was still present after 3 hour-irradiation. A significant protection against photodegradation was observed only when CU was loaded in TS-SLNs, probably because a thick and compact SLN surface layer shielded CU from the external environment. The possibility of the nanoparticulate lipid system to act as physical sunscreen was already hypothesised in the literature [25]. A significant reduction in CU photodegradation occurred in TS-SLNs, which became less pronounced in C18α-CD SLNs. On the other side, only a slight photoprotective effect (about 10%) was noted when CU was loaded in TC-SLNs, probably because TC, having a lower melting point than TS, imparted to SLNs a less compact structure. Moreover, as reported in the literature [26], even in TC-SLNs, the addition of CD derivatives seems not to further protect CU from photodegradation. In these systems the CD cavity size (different in the α and γ series) did not seem to influence the degradation process: only a little difference (5%) in the degradation rate was observed when comparing α- and γ-CD derivatives – loaded SLNs.

The significant photoprotection of CU observed when it was vehicled in TS-SLNs, is probably due to the higher melting point of TS which conferred compactness and thickness to the resultant SLNs. The addition of CD derivatives probably impaired this effect, so that CU was more exposed to photodegradation.

Curcumin hydrolytic stability

It is well known [27-28] that in aqueous solution at pH>7 CU undergoes a rapid hydrolytic degradation, whose main products have been identified as ferulic acid and its methyl ester The formation of an inclusion complex with CD usually slows down the degradation process. However, in some cases, an increase in degradation rate is observed [29]. In the present work we investigated whether the entrapment of CU into TC- and TS-SLNs could reduce its degradation at pH 7.4, and whether the presence of CD derivatives would affect the results. In Figure 6, hydrolytic degradation

plots are shown. As already evidenced in photostability studies, TS-SLNs offered a higher CU protection from external environment than TC-SLNs. Such protective effect seems not to be influenced in any way by the presence of C18α-CD. On the contrary, a considerable protection was also exerted by TC-SLN containing C11α-□CD, an almost 20% increase of undegraded CU being seen compared to TC-SLNs without CD; in the presence of C10γ-□CD no further protection of CU against hydrolytic degradation was observed.

In vitro transepidermal permeation and skin uptake experiments

In the literature we find several studies on antitumoral and anticarcinogenic effects of CU [30].

The mechanisms by which CU suppresses carcinogenesis has been investigated in several animal tumors, including those affecting skin, colon, lung, duodenum, stomach, esophagus, and oral cavity. The effects of CU on several skin carcinogenesis models yielded promising results: in different studies, the topical application of relatively low doses of CU (20 or 100 nmol) markedly suppressed TPA-induced tumour formation [31]; in a benzo[*a*]pyrene-initiated and TPA-promoted two-stage skin tumorigenesis model, CU reduced the number of tumours per mouse as well as the number of tumour-bearing mice; moreover, dietary administration of 2% turmeric significantly inhibited TPA-induced skin tumour formation in female Swiss mice [32].

In view of the mentioned effects of cutaneously applied CU, in this study we tested permeation through pig ear skin and skin uptake of CU-loaded TC and TS SLNs. As reference, a solution of CU in Myritol®318 was used. Skin accumulation results of SLN suspensions are reported in Figure 7.

The CU reference solution showed a quite negligible transepidermal flux, far below the UV-HPLC detection limit; its skin deposition was also very low (0.71 μg/cm^2). All tested suspensions showed similar results regarding transepidermal flux. On the other hand, for all tested suspensions we observed an enhancement of CU deposition into the skin . This increase was a modest one for TC- and TS-SLN suspension (3.3 and 4.7 μg/cm^2 respectively) but was larger for the TC-C10γ–CD SLN suspension (up to 10.9 μg/cm^2). With CU-loaded TS-C18α-CD SLNs a lower increase in skin deposition was seen (7.8 μg/cm^2), and a still lower one with TC-C11α-CD (5.5 μg/cm^2). The amount of CU accumulated from each SLN suspension is probably related to both SLN-encapsulated and free drug present in the aqueous suspensions. As the encapsulation efficiency ranged from 40 to 75% in different SLNs, it was important to evaluate the skin accumulation due only to actually SLN-encapsulated CU. For this reason, SLNs were repeatedly centrifuged and washed as described in the Methods section, then applied to the skin in their solid form. Results, summarized in Figure 8, show a similar trend in skin accumulation for TC- and TS-SLNs, while the

highest value was seen with TS-C18α-CD SLNs, immediately followed by TC-C10γ-CD SLNs; TC-C11α-CD SLN performed only slightly better than TC-SLN. A different picture appears when CU skin accumulation is reported as percentage of the actual SLN-loaded dose for each SLN type. The percentage of drug accumulation in the skin was 7% for TC and TC-C11α-CD SLNs and rose to 14% for TC-C10γ-CD SLN, to 17% for TS SLN and to 23% for TS-C18α-CD SLN.

These results are difficult to interpret. Two factors probably play a role in determining CU skin accumulation: the amount of CU encapsulated in SLNs and the lipophilicity of the substituted CD. The most significant values of accumulation, expressed as percentages of the loaded amount, were obtained for SLNs containing the longer-chain triglyceride TS on whose lipophilicity was only slightly affected by the addition of a single-chain C18. In the case of TC SLNs, an enhancing effect was seen only in the presence of TC-C10γ□-CD; this would seem to be related to the substitution degree of the CD: probably in skin accumulation the lipophilicity of CD-derivatives also plays an important role: C10γ□-CD, with a degree of substitution equal to 3 is more lipophilic than monosubstituted C11α□-CD. On the contrary, melting of TC at skin temperature and the consequent CU skin deposition, seem not be relevant in determining skin permeation.

CONCLUSION

Main results worth underlining are the actual possibility to use lipidic biocompatible matrixes, such as triglycerides, and lipophilic derivatives of α- and γ–CD in the formulation of SLN applying the solvent-injection technique. Both SLN mean sizes and CU encapsulation efficiency could be dramatically improved when the proper CD-derivative - TG mixture was used in the formulation. Moreover the protection of SLN-loaded CU from hydrolysis and from photodegradation, were promising results in order to propose SLN for dermatologic application of the drug, whose , a natural polyphenol obtained from *Curcuma longa*, whose when the proper CD-derivative - TG mixture was used in the formulation. diameters below 1 μm, allowing to hypothesize a possible *in vivo* application. On the other hand, owing to the small volume of the inner aqueous phase in a W/O/W system, and to a non-negligible permeability of both interfaces, great difficulties are still present in encapsulating high percentages of insulin, even if fair concentrations of the peptide are reached as a consequence of the acidic medium.

Further efforts are therefore necessary to improve the encapsulation efficiency in order to propose multiple emulsion-derived SLN for preliminary *in vivo* studies.

ACKNOWLEDGMENTS

This work was supported by a grant from the Italian Government (MIUR, Cofin 2006).

REFERENCES

[1] Ammon, H.P., Wahl, M.A.: Pharmacology of Curcuma Longa. Planta Medica 57, 1-7 (1991)

[2] Maheshwari, R.K., Singh, A.K., Gaddipati, J., Srimal, R.C.: Multiple biological activities of curcumin: a short review. Life Sci. 78, 2081-2087 (2006)

[3] Aggarwal, B.B., Kumar, A., Bharti, A.C.: Anticancer potential of curcumin: preclinical and clinical studies. Anticancer Res. 23, 363-398 (2003)

[4] Bush, J.A.; Cheung K-J.J.; Li G.: Curcumin Induces Apoptosis in Human Melanoma Cells through a Fas Receptor/Caspase-8 Pathway Independent of p53. Exp. Cell. Res. 271, 305-314 (2001)

[5] Lin, J.K., Pan, M.H., Shiau, S.Y.L.: Recent studies on the biofunctions and biotransformations of curcumin. Biofactors 13, 153-158 (2000)

[6] Pfeiffer, E., Hohle, S., Solyom, A., Metzler, M.: Studies on the stability of turmeric constituents. J. Food Eng. 56, 257-259 (2003)

[7] Anand, P., Kunnumakkara, A.B., Newman, R.A., Aggarwal, B.B.: Bioavailability of curcumin: problems and promises. Mol. Pharm. 4, 807-818 (2007)

[8] Tiyaboonchai, W., Tungpradit, W., Plianbangchang, P.: Formulation and characterization of curcuminoids loaded solid lipid nanoparticles. Int. J. Pharm. 337, 299-306 (2007)

[9] Li, L., Braiteh, F.S., Kurzrock, R.: Liposome-encapsulated curcumin: in vitro and in vivo effects on proliferation, apoptosis, signaling and angiogenesis. Cancer 104 (6), 1322-1331 (2005)

[10] Suresh, D., Srinivasan, K.. Studies on the in vitro absorption of spice principles-curcumin, capsaicin,and piperine in rat intestines. Food Chem. Toxicol 45, 1437-1442 (2007)

[11] Ma, Z., Haddadi, A., Molavi, O., Lavasanifar, A., Lai, R., Samuel, J.: Micelles of poly(ethylene oxide)-β-poly(epsilon-caprolactone) as vehicles for the solubilization, stabilization, and controlled delivery of curcumin. J. Biomed. Mater. Res. A 86, 300-310 (2008)

[12] Tønnesen, H., Masson, M., Loftsson, T.: Studies of curcumin and curcuminoids. XXVII. Cyclodextrin complexation: solubility, chemical and photochemical stability. Int. J. Pharm. 244, 127-135 (2002)

[13] Roux, M., Perly, B., Djedaïni-Pilard, F.: Self assemblies of amphiphilic cyclodextrins. Eur. Biophys. J. 36, 861-867 (2007)

[14] Vico, R. V., Silva, O. F., De Rossi, R. H., Maggio, B.: Molecular Organization, Structural Orientation, and Surface Topography of Monoacylated β-Cyclodextrins in Monolayers at the Air-Aqueous Interface. Langmuir 24, 7867-7874 (2008)

[15] Trotta, F., Moraglio, G., Marzona, M., Maritano, S.: Acyclic carbonates of β-cyclodextrin" Gazzetta Chimica Italiana 123, 559-562 (1993)

[16] Franz, T.J.: The percutaneous absorption on the relevance of in vitro data. J. Invest. Dermatol. 190-195 (1975)

[17] Beck, H., Bracher, M.: Protocollo standard: assorbimento/penetrazione percutaneo/a "in vitro" con pelle suina. Acta Technologiae et Legis Medicamenti 2, 123-134 (1991)

[18] Tong, L. H., Hou, Z. J., Inoue, Y., Tai, A.: Molecular recognition by modified cyclodextrins. Inclusion complexation of β-cyclodextrin 6-O-monobenzoate with acyclic and cyclic hydrocarbons. J. Chem. Soc. Perkin Trans. 2, 1253–1257 (1992)

[19] Rao, C. T., Lindberg, B., Lindberg, J., Pitha, J.: Substitution in beta-cyclodextrin directed by basicity: preparation of 2-O-and 6-O-[(R)-and (S)-2-hydroxypropyl] derivatives. J. Org. Chem. 56, 1327–1329 (1991)

[20] Xiao, Y., Wu, Q., Wanga, N., Lin, X. : Regioselective monoacylation of cyclomaltoheptaose at the C-2 secondary hydroxyl groups by the alkaline protease from Bacillus subtilis in nonaqueous media. Carbohydr. Res. 339, 1279-1283 (2004)

[21] Cavalli, R., Trotta, F., Carlotti, M.E., Possetti, B., Trotta, M.: Nanoparticles derived from amphiphilic γ-cyclodextrins. J. Incl. Phenom. Macrocycl. Chem. 57, 657-661 (2007)

[22] Siekmann, B., Westesen, k.: Thermoanalysis of the recrystallization process of melt-homogenized glyceride nanoparticles. Colloids Surf. B 3, 159-175 (1994)

[23] Weber, W.M., Hunsaker, L.A., Abcouwer, S.F., Deck, L.M., Vander Jagt, D.L.: Auto-oxidant activities of curcumin and related enones. Bioorg. Med. Chem. 13, 3811-3820 (2005)

[24] Srinivasan, M., Rajendra Prasad, N., Menon, V.P.: Protective effect of curcumin on γ-radiation induced DNA damage and lipid peroxidation in cultured human lymphocytes. Mutat. Res. 611, 96-103 (2006)

[25] Müller, R.H., Radtke, M., Wissing, S.A.: Solid lipid nanoparticles (SLN) and nanostructured lipid carriers (NLC) in cosmetic and dermatological preparations. Adv. Drug Deliv. Rev 54, 131-155 (2002)

[26] Loftsson, T., Brewster, M.E.: Pharmaceutical applications of cyclodextrins. 1. Drug solubilization and stabilization. J. Pharm. Sci. 85, 1017-1024 (1996)

[27] Tønnesen, H.H., Karlsen, J.: Studies on curcumin and curcuminoids. VI. Kinetics of curcumin degradation in aqueous solution. Z. Lebensm.-Unters.-Forsch. 180, 402-404 (1985)

[28] Tønnesen, H.H., Karlsen, J.: Studies on curcumin and curcuminoids. V. Alkaline degradation of curcumin. Z. Lebensm.-Unters.-Forsch. 180, 132-134 (1985)

[29] Loftsson, T., Brewster, M.E.: Pharmaceutical applications of cyclodextrins. 1. Drug solubilization and stabilization. J. Pharm. Sci. 85, 1017-1024 (1996)
[30] Shishodia, S., Chaturvedi, M.M., Aggarwal, B.B.: Role of Curcumin in Cancer Therapy. Curr. Probl. Cancer 31, 243-305 (2007)
[31] Huang, M.T., Ma, W., Yen, P., Xie, J.G., Han, J., Frenkel, K.: Inhibitory effects of topical application of low doses of curcumin on 12-O-tetradecanoylphorbol-13-acetate-induced tumor promotion and oxidized DNA bases in mouse epidermis. Carcinogenesis 18, 83-88 (1997)
[32] Azuine, M.A., Kayal, J.J., Bhide, S.V.: Protective role of aqueous turmeric extract against mutagenicity of direct-acting carcinogens as well as benzo-pyrene induced genotoxicity and carcinogenicity. J. Cancer Res. Clin. Oncol. 118, 447-452 (1992)

Table 1 Mean diameters of TL-γCD derivatives SLNs

TG	C**X**γ-CD	Diameter (nm)	Polydispersity
TL	/	394 ± 21	0.301
TL	6	522 ± 35	0.307
TL	8	588 ± 38	0.319
TL	10	268 ± 16	0.259
TL	12	237 ± 11	0.164
TL	14	417 ± 33	0.282
TL	16	431 ± 37	0.313

Table 2 Mean diameters of TG-γ–CD derivatives SLN

TG	C**X**γ-CD	Diameter (nm)	Polydispersity
TC	/	405 ± 32	0.248
TC	10	260 ± 15	0.137
TC	12	351 ± 18	0.230
TM	/	477 ± 34	0.231
TM	12	509 ± 35	0.189
TM	14	360 ± 16	0.186
TP	/	358 ± 17	0.222
TP	12	692 ± 53	0.232
TP	16	366 ± 20	0.339

Table 3 Mean diameters of TG-α–CD derivatives SLN

TG	CXα-CD	**Diameter (nm)**	**Polydispersity**
TC	/	405 ± 32	0.248
TC	11	312 ± 14	0.248
TC	18	301 ± 13	0.263
TL	/	394 ± 21	0.301
TL	11	615 ± 44	0.318
TL	18α	423 ± 22	0.288
TM	/	477 ± 34	0.231
TM	11	650 ± 64	0.273
TM	18	433 ± 33	0.309
TP	/	358 ± 17	0.222
TP	18	314 ± 15	0.273
TS	/	441 ± 32	0.254
TS	18	370 ± 18	0.282

Table 4 Curcumin entrapment efficiency of TL-γ–CD derivatives SLN

	C**X**γ-CD	**EE (%)**
TL	/	68.04 ± 6.02
TL	6	12.31 ± 4.25
TL	8	22.16 ± 3.78
TL	10	37.24 ± 4.23
TL	12	80.70 ± 6.70
TL	14	62.13 ± 5.60
TL	16	50.16 ± 3.45

Table 5 Curcumin entrapment efficiency of TG-γ–CD derivatives SLNs

TG	C**X**γ-CD	**EE (%)**
TC	/	55.97 ± 5.30
TC	10	75.70 ± 5.40
TC	12	69.40 ± 4.80
TL	/	68.04 ± 6.02
TL	12	80.70 ± 6.70
TM	/	67.84 ± 4.70
TM	12	80.50 ± 6.50
TM	14	85.27 ± 6.20
TP	/	53.30 ± 5.60
TP	12	63.60 ± 5.30
TP	16	83.64 ± 5.20

Table 6 Curcumin entrapment efficiency of TG-α–CD derivatives SLN

TG	C**X**α-CD	EE
TC	/	55.97 ± 5.30
TC	11	74.78 ± 5.23
TC	18	31.90 ± 2.14
TL	/	68.04 ± 4.58
TL	18	53.05 ± 3.87
TM	/	67.84 ± 4.12
TM	18	46.15 ± 2.86
TP	/	65.55 ± 3.98
TP	18	49.37 ± 2.21
TS	/	37.90 ± 1.45
TS	18	61.38 ± 5.21

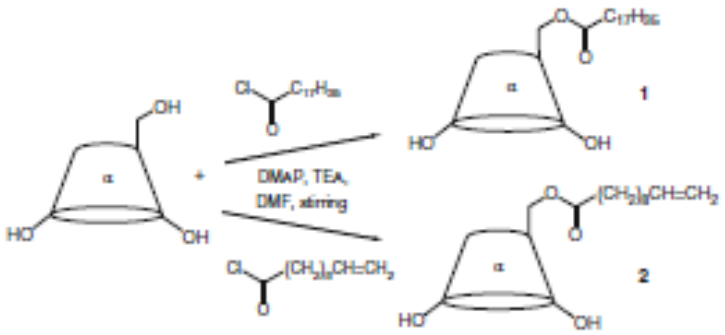

Scheme 1: general scheme of the synthetic procedure

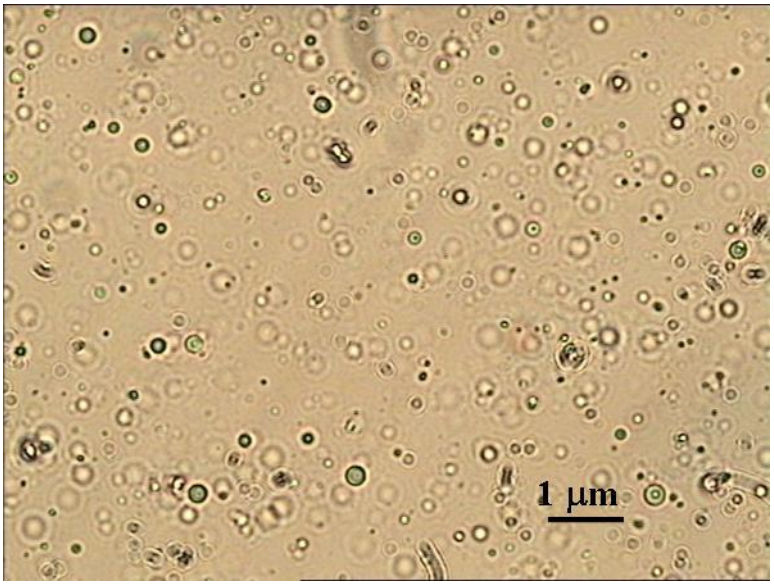

Figure 1a: Micrograph of TL-SLN

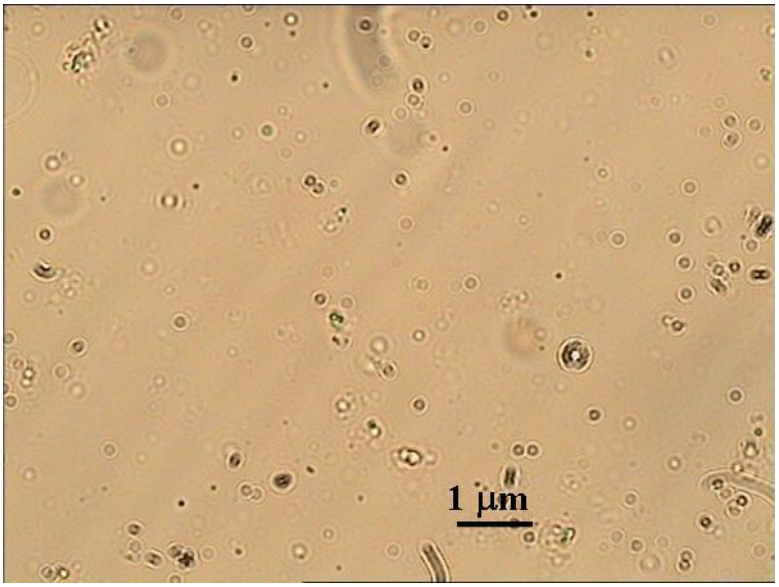

Figure 1b: Micrograph of TL-C12γCD-SLN

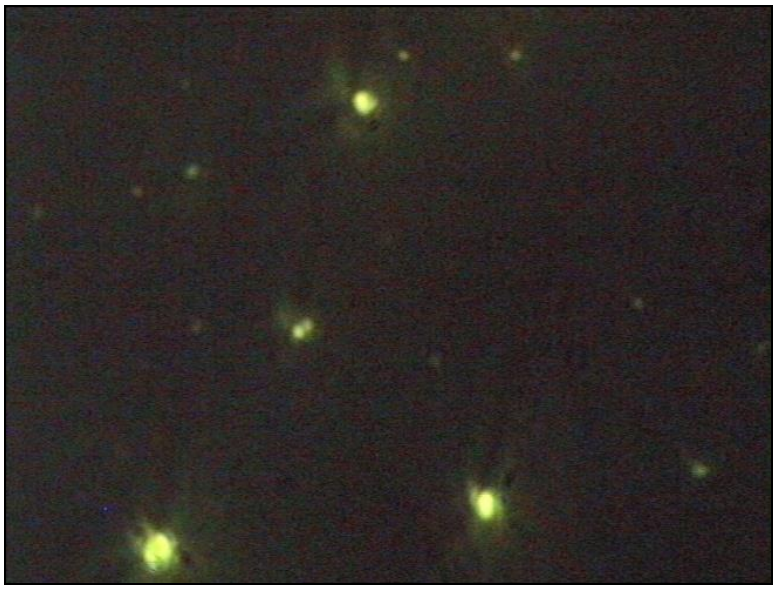

Figure 2a: Micrograph of TL-SLN observed with fluorescent lamp

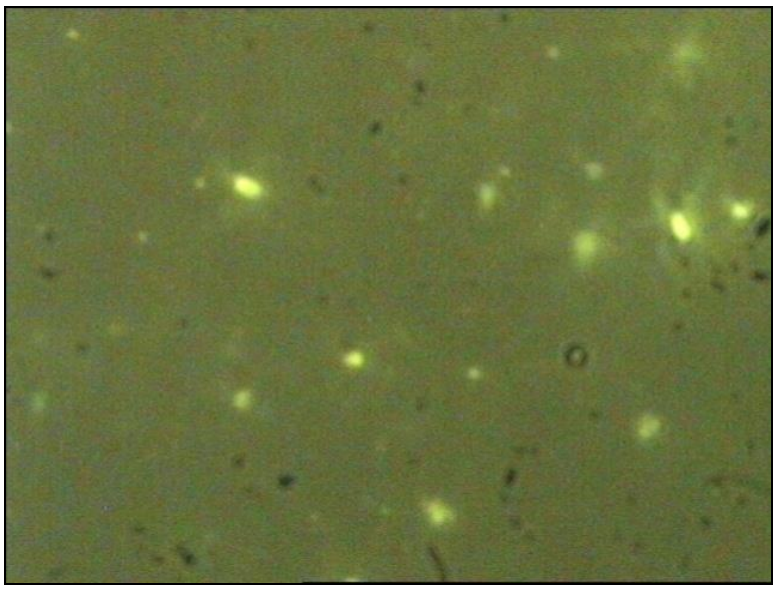

Figure 2b: Micrograph of TL-C12γCD-SLN observed with fluorescent lamp

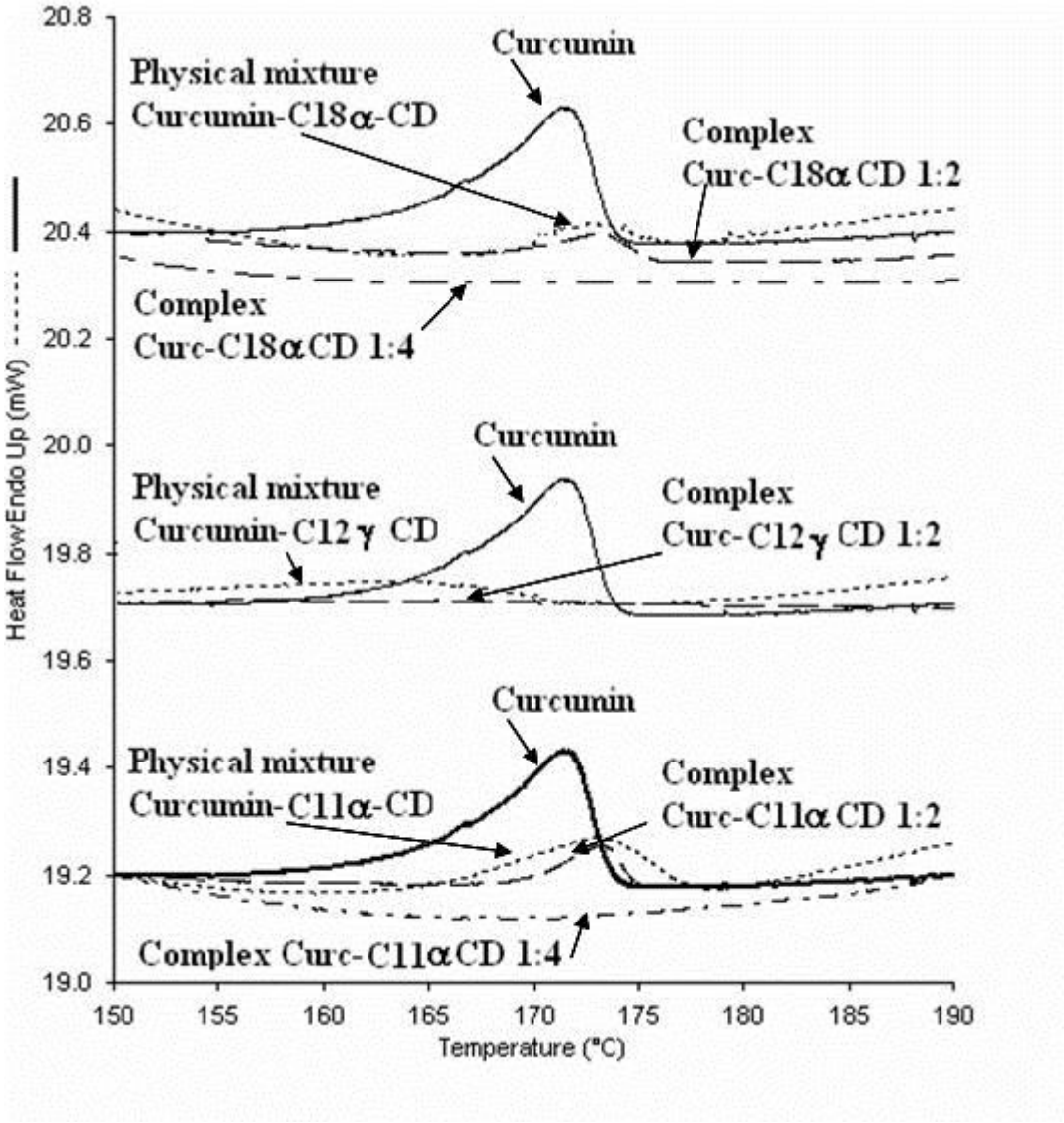

Figure 3: Curcumin DSC thermograms related to complex formation

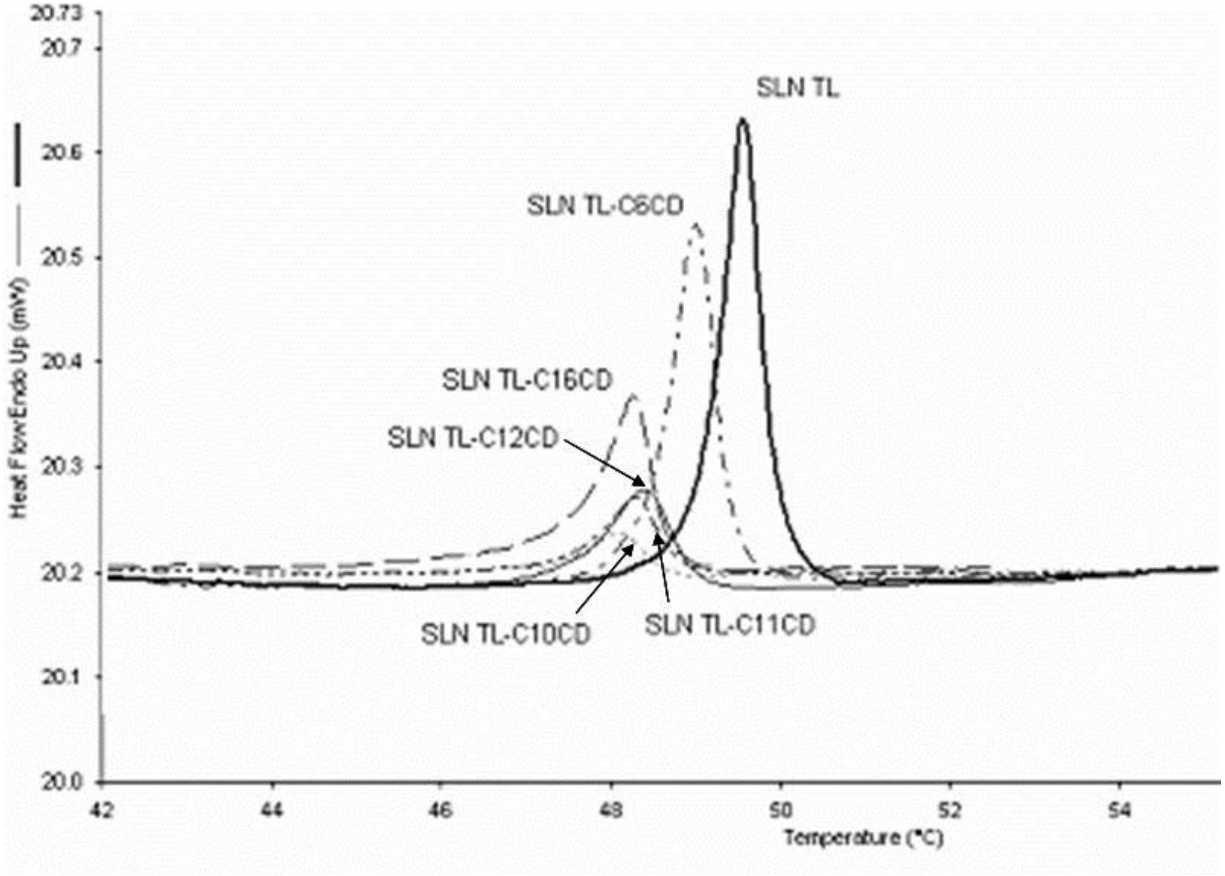

Figure 4: DSC thermograms of different TL-SLN

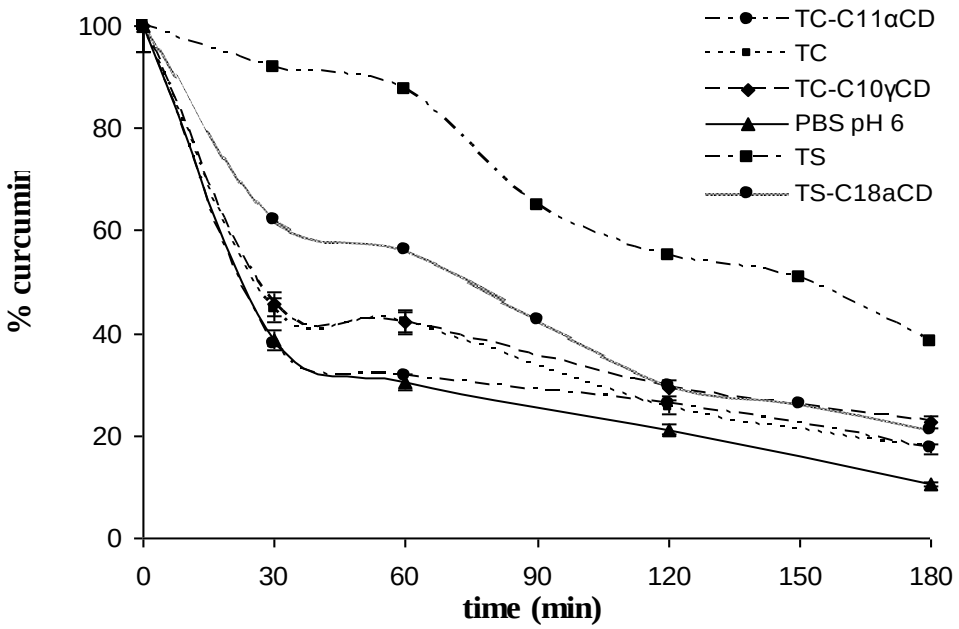

Figure 5: Curcumin UVA photodegradation in aqueous suspension and in different SLNs.

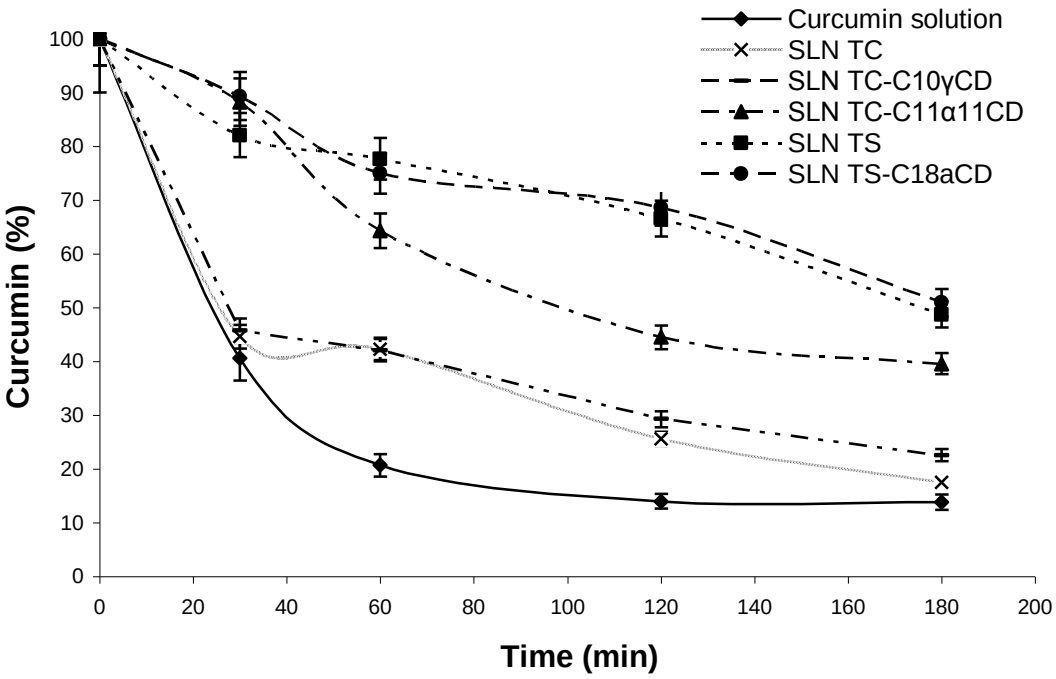

Figure 6: Curcumin hydrolytic degradation in pH 7.4 buffered solution and in different SLNs.

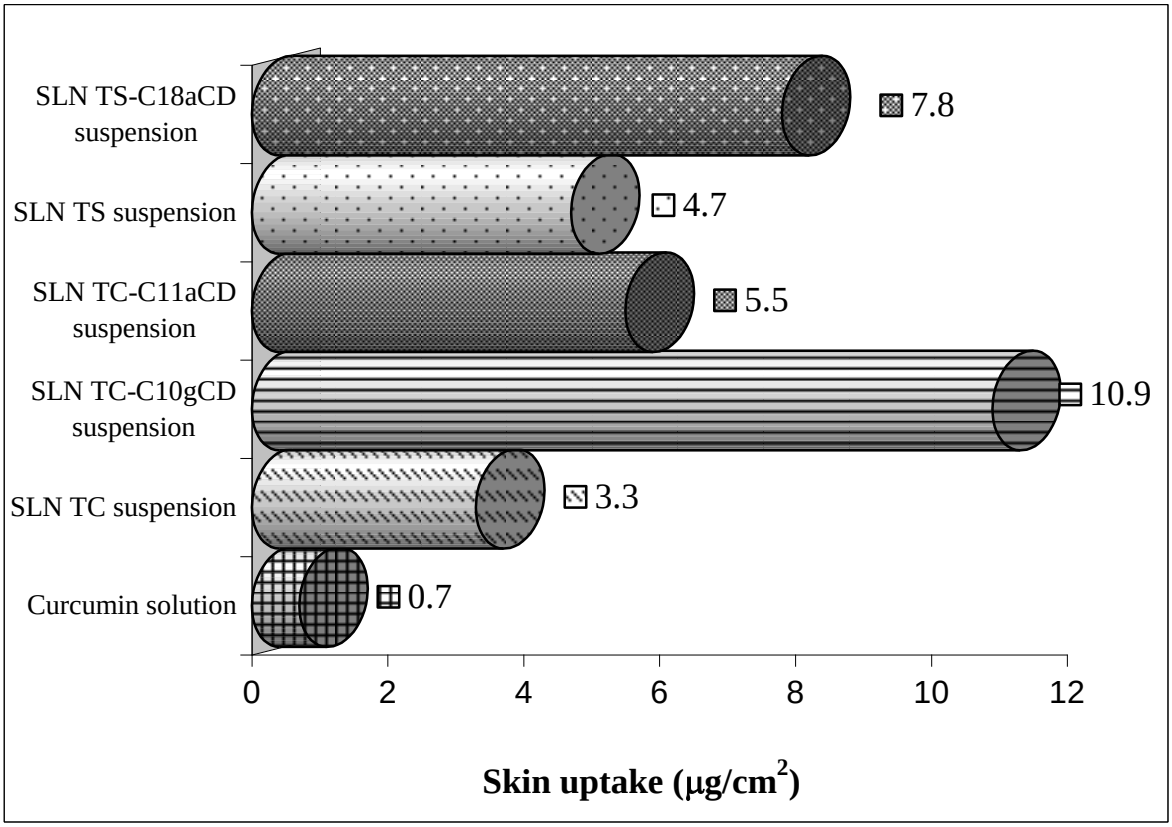

Figure 7: Curcumin skin uptake from different SLN suspension

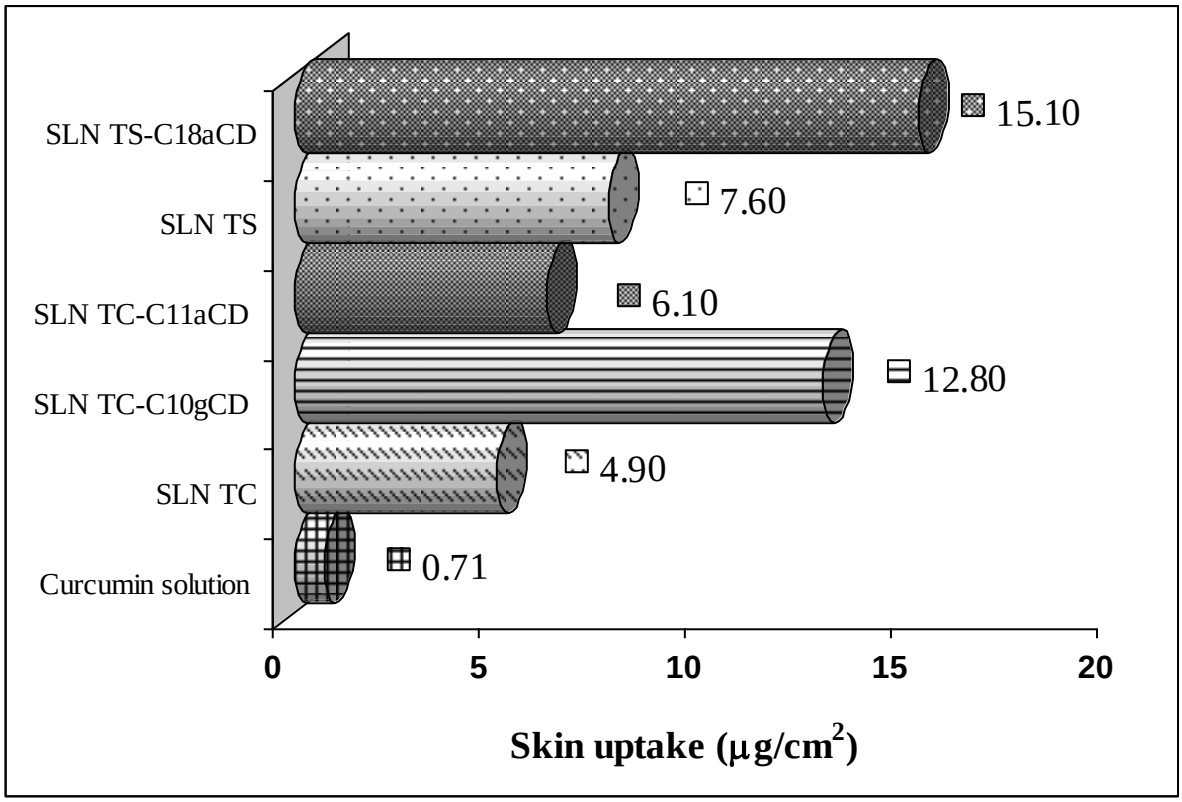

Figure 8: Curcumin skin uptake from different solid SLNs